Fluorination mechanisms of Al_2O_3 and Y_2O_3 surfaces irradiated by high-density CF_4/O_2 and SF_6/O_2 plasmas

Kazuhiro Miwa[a] and Noriharu Takada
Department of Electrical Engineering and Computer Science, Nagoya University, Nagoya, 464-8603, Japan

Koichi Sasaki
Plasma Nanotechnology Research Center, Nagoya University, Nagoya 464-8603, Japan

(Received 17 October 2008; accepted 9 March 2009; published 29 June 2009)

Fluorination of Al_2O_3 and Y_2O_3 surfaces was investigated by irradiating high-density, helicon-wave CF_4/O_2 and SF_6/O_2 plasmas. The Al_2O_3 surface bombarded by high-flux positive ions of the CF_4/O_2 plasma was fluorinated significantly. On contrast, Y_2O_3 was less fluorinated than Al_2O_3 when they were irradiated by the same CF_4/O_2 plasma. The analysis of the Al_2O_3 surface irradiated by the CF_4/O_2 plasma suggests that the fluorination is triggered by reactions between fluorocarbon deposit and Al–O bonding with the assistance of ion bombardment. On the other hand, irradiation of the SF_6/O_2 plasma induced less significant fluorination on the Al_2O_3 surface. This suggests a lower reaction probability between sulfur fluoride deposit and Al–O bonding. The difference in the fluorination of the Al_2O_3 and Y_2O_3 surfaces induced by the irradiations of the CF_4/O_2 and SF_6/O_2 plasmas is understood by comparing the bonding energies of C–O, S–O, Al–O, and Y–O. © *2009 American Vacuum Society.* [DOI: 10.1116/1.3112624]

I. INTRODUCTION

Fluorine-based plasmas are widely used for dry etching of semiconductor materials and for dry cleaning of processing chambers in nanometer-scale device fabrication. The plasmas interact with the inner wall materials of processing chambers inevitably, and the interaction leads to process drifts[1,2] and particle generation.[3] Some countermeasure technologies such as carbon-rich coating[4] and $SiCl_4/Cl_2$ dry cleaning[5] have been developed to suppress the negative influences caused by the interaction between fluorine-based plasmas and processing chambers.

Al_2O_3 is a popular plasma-facing inner wall material used in plasma processing tools. However, it is pointed out in mass-production factories that the Al_2O_3 inner walls have problems in significant erosion and particle generation[3,6,7] when they are immersed in fluorine-based plasmas. Recently, replacing Al_2O_3 with Y_2O_3 was tried to reduce the erosion of the inner wall surface and the particle generation in an etching tool.[3] Plasma processing tools in mass production usually employ thin film coatings of Al_2O_3 and Y_2O_3, and it is known that thin films of Al_2O_3 and Y_2O_3 result in rather easy flake off of particles.[7] This may be because the ceramic coatings usually contain defects such as pores and cracks.[8] In spite of the fact that the particle generation from the inner wall material has great influence on the device yield in mass production, the interaction mechanisms between fluorine-based plasmas and plasma-facing ceramic materials have not been examined in detail. Therefore, in many mass-production factories using plasma processing tools, surface conditions of the chamber wall are controlled by empirical methods.

In this study, we investigated the interaction between fluorine-based plasmas and ceramic materials fundamentally. We produced high-density CF_4/O_2 and SF_6/O_2 plasmas having electron densities of the order of 10^{13} cm^{-3} by helicon-wave discharges. We irradiated the plasmas onto Al_2O_3 and Y_2O_3 samples to examine the change in the surface properties. It is known that the change in the surface properties of the ceramic materials used in industrial plasma processing tools is induced by their long-time (usually, more than a few tens of hours) use. The high-density plasma source has an advantage in inducing the change in the surface properties within rather short-time irradiation, which is important for carrying out the fundamental investigation efficiently.

II. EXPERIMENT

A linear apparatus shown in Fig. 1, which was developed originally as a divertor simulator in a nuclear fusion research,[9] was used in this experiment. The plasma source had a uniform magnetic field of 700 G along the cylindrical axis of the vacuum chamber. A rf power supply at 13.56 MHz was connected to a helical antenna wound around a quartz glass tube of 1.6 cm inner diameter. An instantaneous rf power of 2 kW was pulse modulated at 10 Hz with a duty ratio of 50% to avoid the overheating of the plasma source. The partial pressures of CF_4 (or SF_6) and O_2 were 5 and 2 mTorr, respectively. The plasma was confined radially in the downstream chamber by the magnetic field, and the plasma was like a column, as schematically illustrated in Fig. 1.

The plasma column was terminated by an end plate, on which a sample plate (25 mm square, 2 mm thick) of Al_2O_3 or Y_2O_3 was installed. In this experimental arrangement, we obtained sample surfaces irradiated by the plasma column and by the outside plasma simultaneously. In this article, we

[a]Electronic mail: kazuhiro.miwa@spansion.com

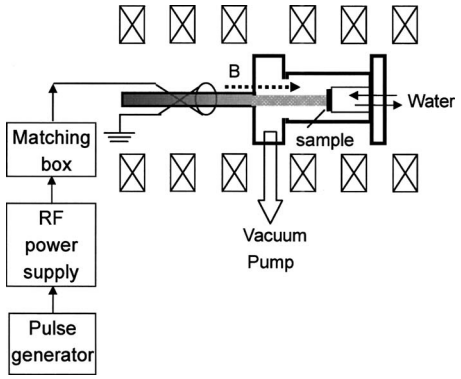

FIG. 1. Schematic of the experimental apparatus.

call the sample region within a radius of 5 mm from the sample center as "center," which was irradiated by the plasma column. The word "outside" in this article means the sample region at a radius from 8 to 12 mm, which was irradiated by the outside plasma. The fluxes of positive ions measured using stainless-steel plates on the sample were 5×10^{15} and 7×10^{14} mm^{-2} s^{-1} in the plasma column and in the outside area, respectively. The irradiation energies of positive ions at the center and at the outside area were estimated to be 50 and 25 eV, respectively, by considering the electron temperatures (6 eV in the plasma column and 1 eV in the outside region[10,11]) and the floating potential (−20 V in both the plasma column and the outside region, which was examined by connecting the stainless-steel plates to a voltage meter with a high input resistance). These irradiation energies are on the same order as those in the actual plasma processing tools. By utilizing the difference in the ion flux and the ion irradiation energy, we examined the contribution of ion bombardment to the change in the surface properties. On the other hand, the fluxes of neutral radicals are expected to be almost uniform in the entire region of the sample since they are not confined by the magnetic field.

The Al_2O_3 and Y_2O_3 plates were fabricated by a sintering process from the pure powders, and the impurity concentrations in the Al_2O_3 and Y_2O_3 samples were less than 0.01% and 0.1% in weight, respectively. The back side of the end plate was connected to a water cooling system to keep the sample temperature constant. The temperature of the sample surface measured using a thermocouple was approximately 600 K during the plasma irradiation when the back side of the end plate was cooled by water. The duration of the plasma irradiation was 2 h for each sample. The surface of the irradiated sample was analyzed by x-ray photoelectron spectroscopy (XPS). The Mg $K\alpha$ line at 1253.6 eV was used as the x-ray source in the XPS system used in this work (Shimazu, ESCA3300).

III. RESULTS

A. Irradiation of CF_4/O_2 plasma

The XPS spectrum of each element on the sample surface was decomposed into components corresponding to chemical

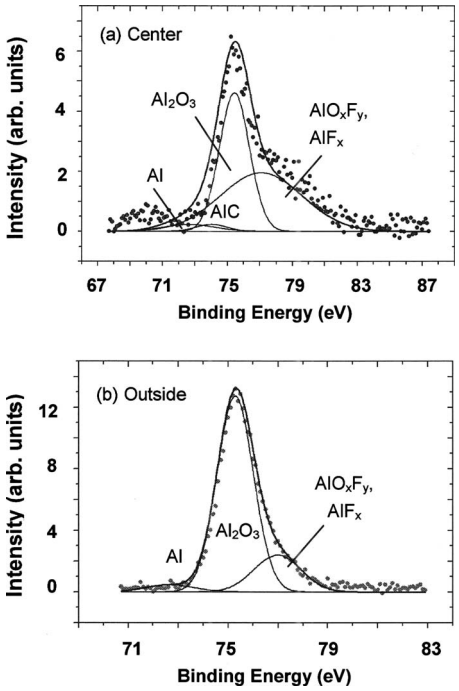

FIG. 2. Spectra of Al 2*p* peaks (a) at the center and (b) in the outside region of the Al_2O_3 sample irradiated by the CF_4/O_2 plasma.

bondings. For example, the Al 2*p* spectra of the Al_2O_3 surface irradiated by the CF_4/O_2 plasma are shown in Fig. 2. Figure 2(a) is the spectrum at the sample center irradiated by the plasma column, while the spectrum in the outside region is shown in Fig. 2(b). The separated peak having the maximum at a binding energy of 75.5 eV corresponds to the Al–O bonding,[12] and this peak dominated the spectrum of a virgin Al_2O_3 sample. We observed an additional peak at 77.3 eV in the spectrum of the irradiated sample, as shown in Fig. 2. This additional peak was assigned to the AlO_xF_y ($x+y=1.5$) and/or AlF_x ($x<3$) (Refs. 12 and 13) bonding components, indicating fluorination of the Al_2O_3 surface by the irradiation of the CF_4/O_2 plasma. In addition, we detected weak peaks corresponding to metallic Al and Al–C bonding[14] on the surface of the Al_2O_3 sample. The Al–C bonding was observed only in the sample irradiated by the plasma column.

We also examined the C 1*s* spectra of the same samples. As a result, the C 1*s* spectrum was separated into C–C, C–F, and $C-F_2$ components, indicating the existence of fluorocarbon polymer layer on the sample surface. We evaluated the relative concentrations of the bonding components by integrating the separated curves. The relative concentrations of metallic Al, fluorinated Al (AlO_xF_y and/or AlF_x), and fluorocarbon on the Al_2O_3 sample irradiated by the CF_4/O_2 plasma are shown in Fig. 3. The relative concentration of fluorocarbon was evaluated by the sum of the C–F and $C-F_2$ components to eliminate the contribution of the C–C peak as impurities to the intensity. Almost the same relative concentration of fluorocarbon was obtained from the integrated intensity of the F 1*s* component. As shown in Fig. 3, the relative concentration of fluorinated Al at the center was three times higher

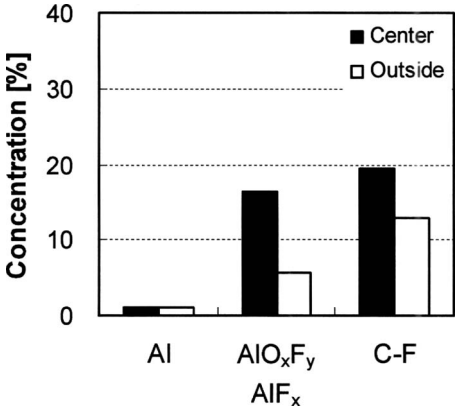

FIG. 3. Relative concentrations of bonding components at the center and in the outside region of the Al_2O_3 sample irradiated by the CF_4/O_2 plasma.

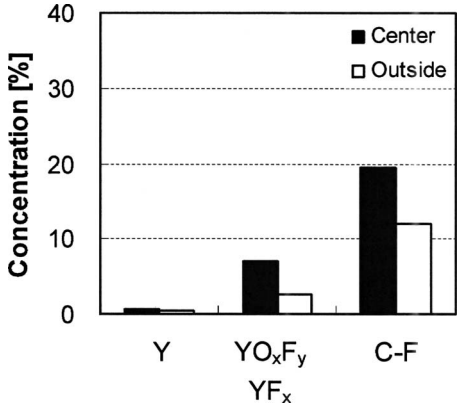

FIG. 5. Relative concentrations of bonding components at the center and in the outside region of the Y_2O_3 sample irradiated by the CF_4/O_2 plasma.

than that in the outside region. In addition, the concentration of fluorocarbon was also higher at the center. The original Al_2O_3 bonding highly survived in the outside area. As has been described in Sec. II, the positive ion flux at the center of the sample was almost seven times higher than that in the outside region. In addition, the irradiation energy of positive ions at the center is estimated to be higher than that in the outside region. Therefore, the experimental result shown in Fig. 3 indicates the contribution of positive ion bombardment to the degradation of the Al_2O_3 surface.

Figures 4(a) and 4(b) show the Y 3*d* spectra at the center and in the outside region of the Y_2O_3 surface irradiated by the CF_4/O_2 plasma, respectively. Although these spectra are more complicated than the Al 2*p* spectra because of the existence of two fine structure components corresponding to

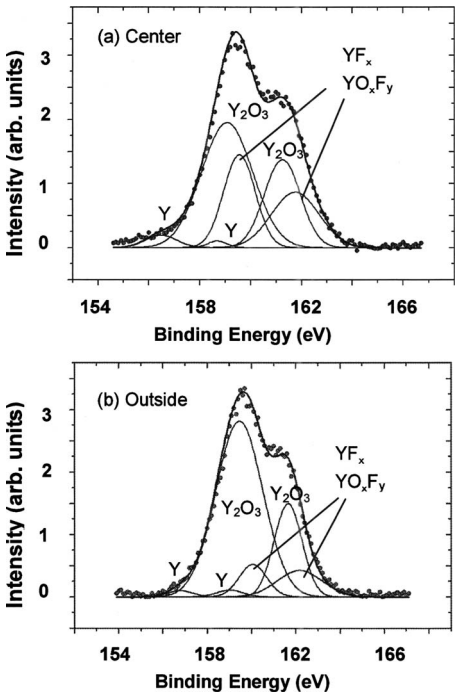

FIG. 4. Spectra of Y 3*d* ($J=5/2,3/2$) peaks (a) at the center and (b) in the outside region of the Y_2O_3 sample irradiated by CF_4/O_2 plasma.

$J=5/2$ and $3/2$ with J being the total angular momentum quantum number, the components induced by the irradiation of the CF_4/O_2 plasma are understood similar to those shown in Fig. 2. The separated peaks at 158.5 and 160.7 eV correspond to the Y–O bonding.[15] The peaks corresponding to the YO_xF_y ($x+y=1.5$) and/or YF_x ($x<3$) (Refs. 1 and 15) components are found at 159.0 and 161.2 eV, indicating the fluorination of the Y_2O_3 surface by the irradiation of the CF_4/O_2 plasma. The appearance of the metallic Y component[11] was also observed on the Y_2O_3 sample.

Figure 5 shows the relative concentrations of metallic Y, fluorinated Y (YO_xF_y and/or YF_x), and fluorocarbon on the Y_2O_3 sample irradiated by the CF_4/O_2 plasma. These concentrations of the bonding components were evaluated by the same way as that used in Fig. 3. Comparing Fig. 5 with Fig. 3, it is known that the relative concentration of fluorocarbon on the Y_2O_3 surface was almost the same as that on the Al_2O_3 surface. In contrast, the relative concentration of fluorinated Y on the Y_2O_3 surface was lower than that on the Al_2O_3 surface, indicating the robustness of Y_2O_3 against the irradiation of the CF_4/O_2 plasma. The contribution of the positive ion bombardment to the fluorination is also seen in the case of the Y_2O_3 sample since the relative concentration of fluorinated Y at the center was higher than that in the outside region.

B. Irradiation of SF_6/O_2 plasma

The Al_2O_3 and Y_2O_3 samples irradiated by the SF_6/O_2 plasma were analyzed by the similar way in evaluating spectra in Figs. 3 and 5. The appearances of the fluorinated (AlO_xF_y, AlF_x, YO_xF_y, and YF_x) and metallic (Al and Y) components were also observed on the Al_2O_3 and Y_2O_3 samples irradiated by the SF_6/O_2 plasma.

Figures 6 and 7 show the relative concentrations of bonding components observed on the Al_2O_3 and Y_2O_3 surfaces irradiated by the SF_6/O_2 plasma, respectively. The relative concentration of sulfur fluoride, which was evaluated from the integrated intensity of the F 1*s* component, was examined instead of fluorocarbon in Figs. 3 and 5. A remarkable difference between the samples irradiated by the CF_4/O_2 and

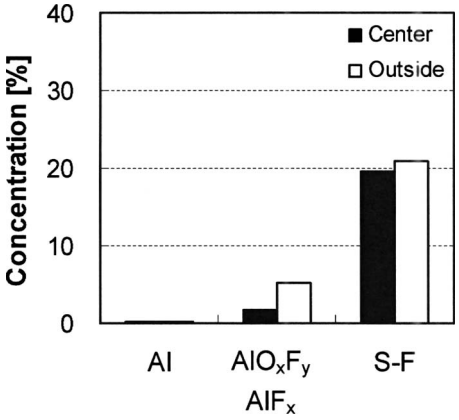

FIG. 6. Relative concentrations of bonding components at the center and in the outside region of the Al_2O_3 sample irradiated by the SF_6/O_2 plasma.

SF_6/O_2 plasmas was found in comparison between the bonding components at the center and in the outside regions.

On the Al_2O_3 and Y_2O_3 surfaces irradiated by the SF_6/O_2 plasma, as shown in Figs. 6 and 7, the relative concentration of sulfur fluoride at the center was roughly equal to that in the outside region. The relative concentration of fluorinated Y at the center of the Y_2O_3 surface was also roughly the same as that in the outside region. The relative concentration of fluorinated Al at the center of the Al_2O_3 surface was lower than that in the outside region. These results were considerably different from the results observed by irradiating the CF_4/O_2 plasma onto the Al_2O_3 and Y_2O_3 samples. Another difference was that the relative concentration of fluorinated Al on the Al_2O_3 sample irradiated by the SF_6/O_2 plasma was lower than that irradiated by the CF_4/O_2 plasma. In addition, the relative concentration of fluorinated Y induced at the center of the Y_2O_3 sample irradiated by the SF_6/O_2 plasma was slightly lower than that irradiated by the CF_4/O_2 plasma, as shown in Figs. 5 and 7.

IV. DISCUSSION

The difference in the relative concentrations of fluorinated Al induced by the irradiations of the CF_4/O_2 and SF_6/O_2 plasmas onto the Al_2O_3 sample, as shown in Figs. 3 and 6, respectively, suggests that the fluorination of Al_2O_3 is triggered by reactions between fluorocarbon deposit and the Al–O bonding. Figure 8 shows a conceptual picture of the fluorination mechanism. The first step is the deposition of a fluorocarbon film due to the adsorption of CF_x radicals in the CF_4/O_2 plasma on the Al_2O_3 surface. It is noted here that the fluorocarbon film illustrated in Fig. 8 is schematic, and we have no quantitative knowledge on the thickness of the fluorocarbon film. The second step is reactions between carbon in the fluorocarbon film and oxygen of the Al–O to form volatile CO, resulting in the decomposition of the Al–O bonding. The AlO_xF_y and/or AlF_x bondings are formed in the third step by reactions between fluorine in the fluorocarbon film and the decomposed Al–O bonding. A part of AlF_3 produced in the third step may desorb from the surface. In addition, it is a bit surprising that metallic Al is left, as shown in Fig. 3. It is apparent that the fluorination via the aforementioned processes is enhanced by bombardment of positive ions since the fluorination at the center of the Al_2O_3 sample was more significant than that in the outside region, as shown in Fig. 3. Accordingly, the fluorination mechanism of Al_2O_3 by the irradiation of the CF_4/O_2 plasma is considered to be similar to the mechanism of reactive ion etching of SiO_2 using fluorocarbon plasmas. The fluorination mechanism of Y_2O_3 by the irradiation of the CF_4/O_2 plasma may be similar to that of Al_2O_3, and the less significant fluorination of Y_2O_3 (Fig. 5) than Al_2O_3 (Fig. 3) is explained by comparing the bonding energies of Y–O [685 kJ/mol (Ref. 16)] and Al–O [512 kJ/mol (Ref. 11)]. Since the bonding energy of Y–O is greater than that of Al–O, reactions between the Y–O bonding and the fluorocarbon deposit is less efficient, resulting in the less significant fluorination of Y_2O_3 than Al_2O_3.

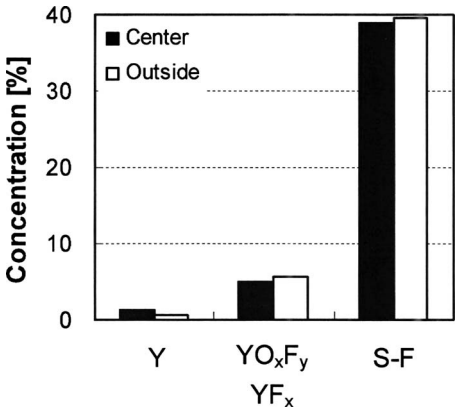

FIG. 7. Relative concentrations of bonding components at the center and in the outside region of the Y_2O_3 sample irradiated by the SF_6/O_2 plasma.

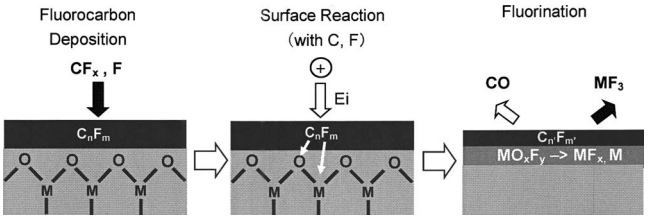

FIG. 8. Conceptual picture of the fluorination mechanism of ceramic surfaces irradiated by fluorine-based plasmas.

The less significant fluorination of the Al_2O_3 sample irradiated by the SF_6/O_2 plasma (Fig. 6) than that by the CF_4/O_2 plasma (Fig. 3) is also understood by comparing the bonding energies. The bonding energy of S–O [549 kJ/mol (Ref. 17)] is smaller than that of C–O [1077 kJ/mol (Ref. 11)]. Since the bonding energy of S–O is close to that of Al–O, the decomposition of the Al–O bonding by reactions with sulfur fluoride deposit may be less efficient than that with fluorocarbon deposit, resulting in the less significant fluorination of Al_2O_3 by the SF_6/O_2 plasma.

The decomposition of the Y–O bonding by reactions with sulfur-fluoride deposit is expected to be more inefficient be-

cause of the higher bonding energy of Y–O than that of S–O. This may be the reason why the high sulfur fluoride concentration close to 40% is observed on the Y_2O_3 surface irradiated by the SF_6/O_2 plasma, as shown in Fig. 7. Another parameters that should be considered here are the boiling temperatures of AlF_3 (1275 °C) and YF_3 (2230 °C). Desorption of YF_3 is expected to be less significant than that of AlF_3 because of the higher boiling point. The low concentration of fluorinated Al at the center of the Al_2O_3 sample irradiated by the SF_6/O_2 plasma (Fig. 6) could be explained by more significant desorption of AlF_3 from the surface.

The experimental results shown in Figs. 6 and 7 suggest that bombardment of positive ions does not enhance the fluorination in the SF_6/O_2 plasma irradiation, which is a different result from that observed by the CF_4/O_2 plasma irradiation. A possible explanation for this difference is the domination of the reaction rate by the flux of F atoms in the case of the SF_6/O_2 plasma irradiation since a higher F atom density is expected in the SF_6/O_2 plasma than in the CF_4/O_2 plasma.

V. CONCLUSIONS

In this work, we compared the degree of fluorination induced on Al_2O_3 and Y_2O_3 surfaces by the irradiations of high-density CF_4/O_2 and SF_6/O_2 plasmas. The major experimental results are (1) Y_2O_3 is more robust than Al_2O_3 against the irradiation of the CF_4/O_2 plasma, and (2) the fluorination by the irradiation of the SF_6/O_2 plasma was less significant than that by the CF_4/O_2 plasma. These results are understood reasonably by considering the difference among the bonding energies of Al–O, Y–O, C–O, and S–O.

The key step in the fluorination process is considered to be the decomposition of the Al–O (or Y–O) bonding on the ceramic surface by reactions with carbon in fluorocarbon deposit (or surfer in surfer fluoride deposit). Once the metal-oxide bonding is decomposed, the progress of fluorination may be inevitable. Hence, the combination between the inner wall material of a plasma processing tool and the dry cleaning gas should be chosen by considering this point of view.

ACKNOWLEDGMENTS

The authors are grateful to Covalent Materials Corporation for providing the ceramics samples used in this work.

[1]G. Cunge, B. Pelissier, O. Joubert, R. Ramos, and C. Maurice, Plasma Sources Sci. Technol. **14**, 599 (2005).
[2]K. Miwa and T. Mukai, J. Vac. Sci. Technol. B **20**, 2120 (2002).
[3]K. Miwa, T. Sawai, M. Aoyama, F. Inoue, A. Oikawa, and K. Imaoka, Proceedings of the IEEE, International Symposium on Semiconductor Manufacturing, Paper No. PO-O-210, p. 479 (2007).
[4]R. Ramos, G. Cunge, O. Joubert, N. Sadeghi, M. Mori, and L. Vallier, Thin Solid Films **515**, 4846 (2007).
[5]R. Ramos, G. Cunge, B. Pelissier, and O. Joubert, Plasma Sources Sci. Technol. **16**, 711 (2007).
[6]S. Y. Mun, K. C. Shin, S. S. Lee, J. S. Kwak, J. Y. Jeong, and Y. H. Jeong, Jpn. J. Appl. Phys., Part 1 **44**, 4891 (2005).
[7]N. Ito, T. Moriya, F. Uesugi, M. Matsumoto, S. Liu, and Y. Kitayama, Jpn. J. Appl. Phys., Part 1 **47**, 3630 (2008).
[8]O. Amsellem, K. Madi, F. Borit, D. Jeulin, V. Guipont, M. Jeandin, E. Boller, and F. Pauchet, J. Mater. Sci. **43**, 4091 (2008).
[9]M. Aramaki, K. Kato, M. Goto, S. Muto, S. Morita, and K. Sasaki, Jpn. J. Appl. Phys., Part 1 **43**, 1164 (2004).
[10]D. Hayashi, M. Nakamoto, N. Takada, K. Sasaki, and K. Kadota, Jpn. J. Appl. Phys., Part 1 **38**, 6084 (1999).
[11]M. A. Lieberman and A. J. Lichtenberg, *Principals of Plasma Discharges and Materials Processing*, 2nd ed. (Wiley, Hoboken, 2005).
[12]Xi Li, Xuefeng Hua, Li Ling, G. S. Oehrlein, E. Karwacki, and Bing Ji, J. Vac. Sci. Technol. A **22**, 158 (2004).
[13]D. S. Kim, Y. Y. Yu, and K. Char, J. Appl. Phys. **96**, 2278 (2004).
[14]C. Hinnen, D. Imbert, J. M. Siffre, and P. Marcus, Appl. Surf. Sci. **78**, 219 (1994).
[15]National Institute of Standards and Technology, Gaithersburg, 2003 NIST X-ray Photoelectron Spectroscopy Database, Version 3.5 (http://srdata.nist.gov/xps/).
[16]M. R. Sievers, Yu-Min Chen, and P. B. Armentrout, J. Chem. Phys. **105**, 6322 (1996).
[17]*Handbook of Chemistry*, Basic 4th ed., edited by The Chemical Society of Japan (Maruzen, Tokyo, 1993) (Kagaku Binran in Japanese).